

# Calix[4]arene-Based 1,3-Diconjugate of Salicylyl Imine Having Dibenzyl Amine Moiety (L): Synthesis, Characterization, Receptor Properties toward $\text{Fe}^{2+}$ , $\text{Cu}^{2+}$ , and $\text{Zn}^{2+}$ , Crystal Structures of Its $\text{Zn}^{2+}$ and $\text{Cu}^{2+}$ Complexes, and Selective Phosphate Sensing by the [ZnL]

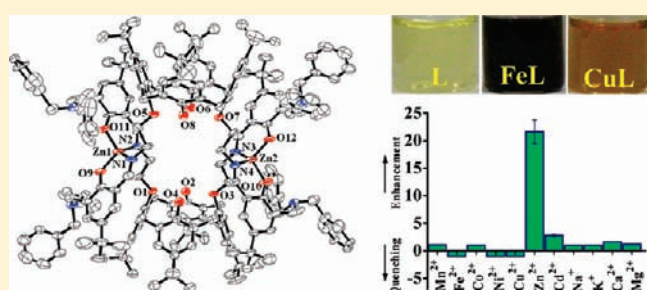
Roymon Joseph, Jugun Prakash Chinta, and Chebrolu P. Rao\*

Bioinorganic Laboratory, Department of Chemistry, Indian Institute of Technology Bombay, Mumbai 400 076, India

## Supporting Information

**ABSTRACT:** A calix[4]arene conjugate bearing salicylyl imine having dibenzyl moiety (L) has been synthesized and characterized, and its ability to recognize three most important essential elements of human system, viz., iron, copper, and zinc, has been addressed by colorimetry and fluorescence techniques. L acts as a sensor for  $\text{Cu}^{2+}$  and  $\text{Fe}^{2+}$  by exhibiting visual color change and for  $\text{Zn}^{2+}$  based on fluorescence spectroscopy. L shows a minimum detection limit of  $3.96 \pm 0.42$  and  $4.51 \pm 0.53$  ppm and  $45 \pm 4$  ppb, respectively, toward  $\text{Fe}^{2+}$ ,  $\text{Cu}^{2+}$ , and  $\text{Zn}^{2+}$ . The in situ prepared [ZnL] exhibits phosphate sensing among 14 anions studied with a detection limit of  $247 \pm 25$  ppb.

The complexes of  $\text{Zn}^{2+}$ ,  $\text{Cu}^{2+}$ , and  $\text{Fe}^{2+}$  of L have been synthesized and characterized by different techniques. The crystalline nature of the zinc and copper complexes and the noncrystalline nature of simple L and its iron complex have been demonstrated by powder XRD. The structures of  $\text{Cu}^{2+}$  and  $\text{Zn}^{2+}$  complexes have been established by single crystal XRD wherein these were found to be 1:1 monomeric and 2:2 dimeric, respectively, using  $\text{N}_2\text{O}_2$  as binding core. The geometries exhibited by the  $\text{Zn}^{2+}$  and the  $\text{Cu}^{2+}$  complexes were found to be distorted tetrahedral and distorted square planar, respectively. The iron complex of L exists in 1:1 stoichiometry as evident from the mass spectrometry and elemental analysis.



## INTRODUCTION

Transition metal ions of iron, copper, and zinc<sup>1</sup> are essential for life by being present in the active sites of numerous enzymes followed by exhibiting a variety of biological functions.<sup>2</sup> While the zinc is involved mainly in hydrolytic type reactions<sup>3</sup> and DNA replication,<sup>4</sup> the iron and the copper are involved in a number of oxido-reductase<sup>5</sup> as well as electron transfer<sup>6</sup> processes owing to their existence in more than one oxidation state in biology. While the zinc's metabolic disorder results in neurological diseases like Alzheimer<sup>7</sup> and epilepsy,<sup>8</sup> the accumulation of copper is toxic and it can even cause liver damage in children.<sup>9</sup> Inefficient iron transport is the main cause of anemia<sup>10</sup> in human, while excess accumulation results in cardiomyopathic, arthropathic, and neurodegenerative disorders.<sup>11</sup> Similar to cations, the detection and quantification of anions is challenging due to the special features exhibited by anions, viz., geometry and shape variation, high energy of solvation, etc.<sup>12</sup> Sensing of phosphates and its derivatives is important in biology owing to its involvement in various biochemical processes such as signal transduction and energy storage.<sup>13</sup> Therefore, it is necessary to develop receptors which can selectively detect such ions of essential trace elements and biologically relevant anions by spectroscopy. It will be more advantageous if the receptor can show visually detectable color changes in the presence of such ions. Supramolecular systems

like calix[4]arene<sup>14</sup> can provide a platform where one can append different binding moieties at its lower rim via various chemical reactions thereby attaining a preorganized binding core toward metal ions. A number of functionalized calix[4]arenes have been used in the literature for the selective detection of ions,<sup>15</sup> molecular species,<sup>16</sup> and metalloenzyme models.<sup>17</sup> Though some reports are available for the selective detection of  $\text{Zn}^{2+}$ ,  $\text{Cu}^{2+}$ , and  $\text{Fe}^{2+}$  by calix[4]arene conjugates,<sup>18</sup> to our knowledge, there is no report in the literature wherein a single system can sense all the three ions. Further, the structural characterization of the species of recognition is rather scarce in the literature.<sup>18h,19</sup> Though there are some metal based anion recognitions reported in the literature,<sup>20</sup> the same for phosphate are rather rare.<sup>18i,21</sup> Recently, our group has been involved in the synthesis of different conjugates of calix[4]arene for studying their selective recognition of biologically relevant metal ions, viz.,  $\text{Zn}^{2+}$ ,  $\text{Cu}^{2+}$ ,  $\text{Ni}^{2+}$ , as well as a toxic ion,  $\text{Hg}^{2+}$ .<sup>18d-f,h,i,t,22</sup> Therefore, in this paper we report the synthesis, characterization of a 1,3-diconjugate of calix[4]arene appended with salicylyl moiety containing a dibenzyl through an imine linker and its receptor properties toward  $\text{Fe}^{2+}$ ,  $\text{Cu}^{2+}$ , and  $\text{Zn}^{2+}$  by absorption and fluorescence spectroscopy,

Received: March 16, 2011

Published: July 01, 2011

and the structure demonstration of the corresponding  $\text{Cu}^{2+}$  and  $\text{Zn}^{2+}$  complexes by single crystal XRD. In addition to this, the phosphate binding of the in situ prepared zinc complex of **L**,  $[\text{ZnL}]$ , has also been demonstrated.

## EXPERIMENTAL SECTION

**General Information and Materials.**  $^1\text{H}$  and  $^{13}\text{C}$  NMR spectra were measured on a Varian Mercury NMR spectrometer working at 400 MHz. The mass spectra were recorded on Q-TOF micromass (YA-105) using electrospray ionization method. Steady state fluorescence spectra were measured on Perkin-Elmer LS55. The absorption spectra were measured on Varian Cary 100 Bio. The elemental analyses were performed on a ThermoQuest microanalysis instrument, and the FT IR spectra were measured on Perkin-Elmer spectrometer using KBr pellets. The diffraction data were collected on OXFORD DIFFRACTION XCALIBUR-S. All the perchlorate salts, viz.,  $\text{Mn}(\text{ClO}_4)_2 \cdot 6\text{H}_2\text{O}$ ,  $\text{Fe}(\text{ClO}_4)_2 \cdot x\text{H}_2\text{O}$ ,  $\text{Co}(\text{ClO}_4)_2 \cdot 6\text{H}_2\text{O}$ ,  $\text{Ni}(\text{ClO}_4)_2 \cdot 6\text{H}_2\text{O}$ ,  $\text{Cu}(\text{ClO}_4)_2 \cdot 6\text{H}_2\text{O}$ ,  $\text{Zn}(\text{ClO}_4)_2 \cdot 6\text{H}_2\text{O}$ ,  $\text{Cd}(\text{ClO}_4)_2 \cdot \text{H}_2\text{O}$ ,  $\text{NaClO}_4 \cdot \text{H}_2\text{O}$ ,  $\text{KClO}_4$ ,  $\text{Ca}(\text{ClO}_4)_2 \cdot 4\text{H}_2\text{O}$ , and  $\text{Mg}(\text{ClO}_4)_2 \cdot 6\text{H}_2\text{O}$ , were procured from Sigma Aldrich Chemical Co. Salts possessing different anions, viz.,  $\text{Bu}_4\text{NF}$ ,  $\text{Me}_4\text{NCl}$ ,  $\text{Bu}_4\text{NBr}$ ,  $\text{Bu}_4\text{NI}$ ,  $\text{Bu}_4\text{NClO}_4$ ,  $\text{Bu}_4\text{NH}_2\text{PO}_4$ ,  $\text{Na}_2\text{HPO}_4$ ,  $\text{Na}_4\text{P}_2\text{O}_7$ ,  $\text{NaSCN}$ ,  $\text{NaOAc}$ ,  $\text{Na}_2\text{SO}_4$ ,  $\text{Na}_2\text{CO}_3$ ,  $\text{NaNO}_3$ , and  $\text{NaBF}_4$ , were purchased from Sisco Research Laboratories Pvt Ltd., India. Bulk solutions of **L** and the metal salts were made in  $\text{CHCl}_3$  and  $\text{MeOH}$ , respectively, at  $6 \times 10^{-4}$  M. All the fluorescence titrations were carried out in 1 cm quartz cells by using  $50 \mu\text{L}$  of **L**, and the total volume in each measurement was made to 3 mL to give a final concentration of the ligand as  $10 \mu\text{M}$  (i.e., the 3 mL solution contains 2.950 mL of  $\text{CH}_3\text{OH}$  and 0.050 mL of  $\text{CHCl}_3$ ). During the titration, the concentration of metal perchlorate was varied accordingly to result in requisite mole ratios of metal ion to **L**, and the total volume of the solution was maintained at 3 mL in each case by addition of  $\text{CH}_3\text{OH}$ . For absorption studies, the final concentration of **L** was kept constant at  $20 \mu\text{M}$ , and the procedure used for the titrations was the same as that used for fluorescence titrations.

**Synthesis and Characterization of 1.** A mixture of *p*-tert-butylcalix[4]arene (1.0 g, 1.55 mmol),  $\text{K}_2\text{CO}_3$  (0.85 g, 6.20 mmol),  $\text{NaI}$  (0.92 g, 6.13 mmol), and chloroacetonitrile (0.4 mL, 5.33 mmol) in 50 mL of acetone was refluxed under nitrogen atmosphere for 7 h. The reaction mixture was allowed to cool down to room temperature and filtered through Celite. The Celite was washed with dichloromethane to obtain light brown clear solution. This was concentrated to give brown solid, which was recrystallized from chloroform/methanol to give white crystalline solid. Yield (900 mg) 80%. Anal. Calcd for  $\text{C}_{48}\text{H}_{58}\text{N}_2\text{O}_4$ : C, 79.30; H, 8.04; N, 3.85. Found: C, 79.49; H, 8.30; N, 3.92%. FTIR (KBr,  $\text{cm}^{-1}$ ): 1482 ( $\nu_{\text{CN}}$ ), 3515 ( $\nu_{\text{OH}}$ ).  $^1\text{H}$  NMR ( $\text{CDCl}_3$ ,  $\delta$  ppm): 0.88, (s, 18H,  $\text{C}(\text{CH}_3)_3$ ), 1.32 (s, 18H,  $\text{C}(\text{CH}_3)_3$ ), 3.45 (d,  $J = 13.55$  Hz, 4H,  $\text{Ar}-\text{CH}_2-\text{Ar}$ ), 4.22 (d,  $J = 13.55$  Hz, 4H,  $\text{Ar}-\text{CH}_2-\text{Ar}$ ), 4.81 (s, 4H,  $\text{OCH}_2$ ), 6.73 (s, 4H,  $\text{Ar}-\text{H}$ ), 7.12 (s, 4H,  $\text{Ar}-\text{H}$ ).

**Synthesis and Characterization of 2.** To a vigorously stirred solution of **1** (0.58 g, 0.81 mmol) in 32 mL of diethyl ether was added  $\text{LiAlH}_4$  (0.25 g, 7.13 mmol), and the reaction mixture was refluxed for 5 h. After that, the reaction flask was immersed into an ice–water bath, and excess  $\text{LiAlH}_4$  was destroyed by the addition of wet benzene into the reaction mixture. The clear organic layer was decanted, and the inorganic salts were rinsed with benzene. The combined organic layers were evaporated to dryness to yield diamine, as a light yellow solid. Yield (470 mg) 85%. Anal. Calcd for  $\text{C}_{48}\text{H}_{66}\text{N}_2\text{O}_4$ : C, 78.43; H, 9.05; N, 3.81. Found: C, 78.29; H, 8.87; N, 3.97%. FTIR (KBr,  $\text{cm}^{-1}$ ): 3362 ( $\nu_{\text{OH/NH}}$ ).  $^1\text{H}$  NMR ( $\text{CDCl}_3$ ,  $\delta$  ppm): 1.10 (s, 18H,  $\text{C}(\text{CH}_3)_3$ ), 1.24 (s, 18H,  $\text{C}(\text{CH}_3)_3$ ), 3.29 (t,  $J = 4.76$ , 4.76 Hz, 4H,  $\text{NCH}_2$ ), 3.37 (d,  $J = 12.82$  Hz, 4H,  $\text{Ar}-\text{CH}_2-\text{Ar}$ ), 4.07 (t,  $J = 4.76$ , 4.76 Hz, 4H,  $\text{OCH}_2$ ), 4.32 (d,  $J = 12.82$  Hz, 4H,  $\text{Ar}-\text{CH}_2-\text{Ar}$ ), 6.97 (s, 4H,  $\text{Ar}-\text{H}$ ), 7.04 (s, 4H,  $\text{Ar}-\text{H}$ ).

$^{13}\text{C}$  NMR ( $\text{CDCl}_3$ , 100 MHz,  $\delta$  ppm): 31.3, 37.8 ( $\text{C}(\text{CH}_3)_3$ ), 34.0, 34.3 ( $\text{C}(\text{CH}_3)_3$ ), 32.3 ( $\text{Ar}-\text{CH}_2-\text{Ar}$ ), 42.7 ( $\text{CH}_2\text{N}$ ), 78.7 ( $\text{OCH}_2$ ), 125.6, 126.0, 127.8, 133.3, 142.2, 147.7, 149.3, 150.4 ( $\text{Ar}-\text{C}$ ). ES MS:  $m/z = 735.26$  ( $\text{M}^+$ , 100%).

**Synthesis and Characterization of L.** A mixture of **2** (0.3 g, 0.43 mmol) and **1c** (0.33 g, 0.85 mmol) were stirred in 50 mL of methanol at room temperature for 12 h, and the yellow precipitate that formed was filtered, washed, and dried under vacuum. Yield (0.33 g, 52%). Anal. Calcd for  $\text{C}_{100}\text{H}_{120}\text{N}_4\text{O}_6 \cdot 3\text{CH}_3\text{OH}$ : C, 78.79; H, 8.47; N, 3.57. Found: C, 78.76; H, 8.10; N, 3.54%. FTIR (KBr,  $\text{cm}^{-1}$ ): 3397 ( $\nu_{\text{OH}}$ ), 1633 ( $\nu_{\text{C=N}}$ ).  $^1\text{H}$  NMR ( $\text{CDCl}_3$ ,  $\delta$  ppm): 0.85 (s, 18H,  $\text{C}(\text{CH}_3)_3$ ), 1.16 (s, 18H,  $\text{C}(\text{CH}_3)_3$ ), 1.19 (s, 18H,  $\text{C}(\text{CH}_3)_3$ ), 3.17 (d, 4H,  $\text{Ar}-\text{CH}_2-\text{Ar}$ ,  $J = 13.8$  Hz), 3.49 (s, 8H,  $\text{Ar}-\text{CH}_2$ ), 3.56 (s, 4H,  $\text{Ar}-\text{CH}_2$ ), 4.00 (t,  $\text{OCH}_2$ , 4H,  $J = 5.5$  Hz), 4.16 (m, 8H,  $\text{Ar}-\text{CH}_2-\text{Ar}$  and  $\text{NCH}_2$ ), 6.67 (s, 4H,  $\text{Ar}-\text{H}$ ), 6.90 (s, 4H,  $\text{Ar}-\text{H}$ ), 7.10–7.33 (m, 24H,  $\text{Ar}-\text{H}$ ), 7.56 (s, 2H,  $\text{Ar}-\text{OH}$ ), 8.53 (s, 2H,  $\text{CH=N}$ ), 13.12 (s, 2H,  $\text{ArOH}$ ).  $^{13}\text{C}$  NMR ( $\text{CDCl}_3$ , 100 MHz,  $\delta$  ppm): 31.2, 31.6, 31.8 ( $\text{C}(\text{CH}_3)_3$ ), 31.4 ( $\text{Ar}-\text{CH}_2-\text{Ar}$ ), 33.9, 34.0, 34.1 ( $\text{C}(\text{CH}_3)_3$ ), 51.2 ( $\text{Ph}-\text{CH}_2-\text{N}$ ), 58.5 ( $\text{NCH}_2$ ), 59.0 ( $\text{NCH}_2\text{CH}_2$ ), 75.5 ( $\text{OCH}_2$ ), 118.1, 125.2, 125.8, 126.3, 126.6, 126.9, 127.9, 128.3, 128.7, 129.0, 129.4, 130.6, 132.5, 140.2, 140.9, 141.5, 147.1, 149.9, 150.7, 157.3 ( $\text{Ar}-\text{C}$ ), 168.0 ( $\text{NCH}$ ). ES MS:  $m/z = 1474$  ( $\text{M}^+$ , 20%).

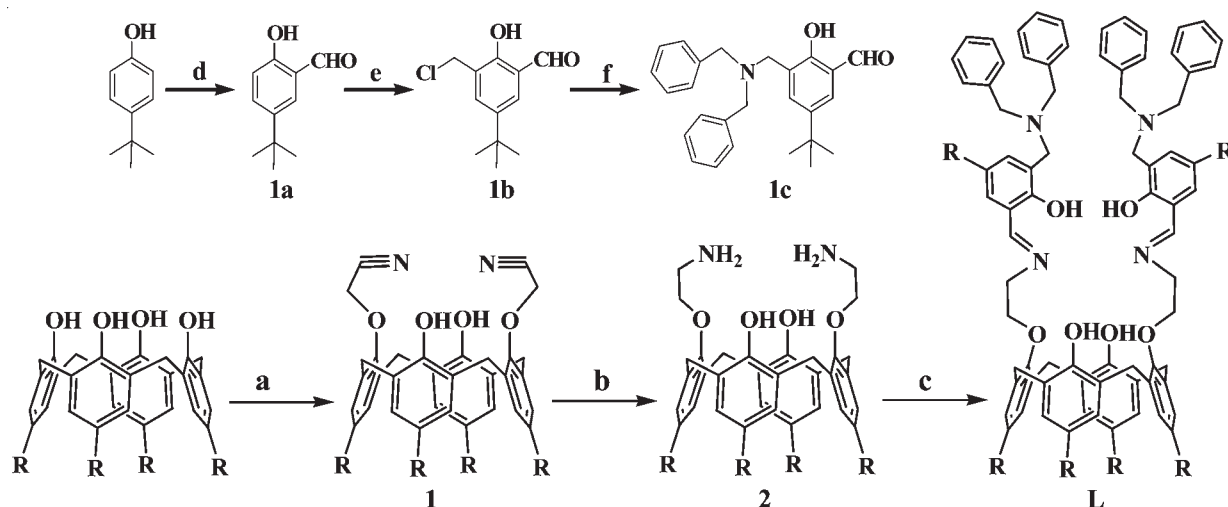
**Synthesis and Characterization of Zinc Complex of L, 3.** To a solution of **L** (0.08 g, 0.05 mmol) in  $\text{CH}_2\text{Cl}_2$  (5 mL) was added zinc(II) acetate (0.013 g, 0.06 mmol) in methanol dropwise. After stirring for one day, the reaction mixture was heated for 5 h at  $40^\circ\text{C}$ . The solvent was evaporated, and the complex was recrystallized from methanol–dichloromethane mixture. Yield (0.063 g, 75%). FTIR (KBr,  $\text{cm}^{-1}$ ): 1616 ( $\nu_{\text{C=N}}$ ), 3388 ( $\nu_{\text{OH}}$ ). Anal. Calcd for  $\text{C}_{200}\text{H}_{236}\text{N}_8\text{O}_{12}\text{Zn}_2$ : C, 78.12; H, 7.74; N, 3.64. Found: C, 78.58; H, 7.50; N, 3.61%.  $^1\text{H}$  NMR ( $\text{CDCl}_3$ , 400 MHz): 1.12 (s, 18H,  $\text{Sal}-(\text{CH}_3)_3$ ), 1.14 (s, 18H,  $(\text{CH}_3)_3$ ), 1.16 (s, 18H,  $(\text{CH}_3)_3$ ), 3.53–3.60 (m, 4H,  $\text{OCH}_2$ ), 3.64 (s, 8H,  $\text{Ar}-\text{CH}_2$ ), 3.67 (s, 4H,  $\text{Ar}-\text{CH}_2$ ), 4.04, 4.01 (bs, 2H,  $-\text{NCH}_2$ ), 4.17, 3.78, 3.46, 2.95 (d,  $J = 12.8$  Hz, 8H,  $\text{Ar}-\text{CH}_2-\text{Ar}$ ), 4.77 (t,  $J = 10.80$ , 10.52 Hz, 2H,  $\text{NCH}_2$ ), 6.74 (d,  $J = 2.64$  Hz, 2H,  $\text{Ar}-\text{H}$ ), 6.85 (s, 4H,  $\text{Ar}-\text{H}$ ), 6.90–6.96 (dd, 4H,  $\text{Ar}-\text{H}$ ), 7.14 (t,  $J = 7.36$ , 7.36 Hz, 4H,  $\text{Ar}-\text{H}$ ), 7.28 (t,  $J = 7.44$ , 8.76 Hz, 8H,  $\text{Ar}-\text{H}$ ), 7.46 (d,  $J = 7.12$  Hz, 8H,  $\text{Ar}-\text{H}$ ), 7.81 (d,  $J = 2.64$  Hz, 2H,  $\text{Ar}-\text{H}$ ), 8.40 (s, 2H,  $\text{Ar}-\text{OH}$ ), 8.44 (s, 2H, imine-H).  $m/z$  (MALDI-TOF) 3074.84 ( $[\text{3}]^+$ ). Single crystals were grown by slow evaporation of **3** in a mixture of chloroform and methanol.

**Synthesis and Characterization of Copper Complex of L, 4.** The copper complex has been synthesized by following the procedure used for the synthesis of zinc complex, viz., by adding copper(II) acetate (0.014 g, 0.07 mmol) to **L** (0.10 g, 0.07 mmol). The complex formed was recrystallized from a mixture of methanol and dichloromethane. Yield (0.07 g, 67%). FTIR (KBr,  $\text{cm}^{-1}$ ): 1620 ( $\nu_{\text{C=N}}$ ), 3438 ( $\nu_{\text{OH}}$ ). Anal. Calcd for  $\text{C}_{100}\text{H}_{118}\text{N}_4\text{O}_6\text{Cu} \cdot \text{CH}_3\text{CN}$ : C, 77.70; H, 7.74; N, 4.44%. Found: C, 77.50; H, 8.07; N, 4.04. ESI MS:  $m/z = 1535.68$  ( $[\text{4}]^+$ ). Single crystals were grown by slow evaporation of **4** taken in acetonitrile.

**Synthesis and Characterization of Iron Complex of L, 5.** The procedure used for the synthesis of iron complex is same as that used for the zinc and copper complex but by adding iron(II) perchlorate (0.017 g, 0.07 mmol) to **L** (0.10 g, 0.07 mmol). The complex formed has been crystallized from a mixture of dichloromethane and methanol; however, no single crystals could be obtained. Yield (0.06 g, 60%). FTIR (KBr,  $\text{cm}^{-1}$ ): 1617 ( $\nu_{\text{C=N}}$ ). Anal. Calcd for  $\text{C}_{100}\text{H}_{118}\text{N}_4\text{O}_6\text{Fe} \cdot \text{CH}_2\text{Cl}_2$ : C, 75.22; H, 7.50; N, 3.47. Found: C, 74.84; H, 7.50; N, 3.44. ESI MS:  $m/z = 1527.73$  ( $[\text{5}]^+$ ).

## RESULTS AND DISCUSSION

The receptor molecule, **L**, has been synthesized by three steps<sup>23</sup> (Scheme 1) starting from *p*-tert-butylcalix[4]arene followed

Scheme 1. Synthesis of the Precursor Molecule 1c and the Receptor Molecule L<sup>a</sup>

<sup>a</sup> Synthesis of the receptor, L: (a)  $\text{K}_2\text{CO}_3$ ,  $\text{ClCH}_2\text{CN}$ , acetone, reflux for 7 h; (b)  $\text{LiAlH}_4$ ,  $\text{C}_2\text{H}_5\text{OC}_2\text{H}_5$ , reflux for 5 h; (c) 3-((dibenzylamino)methyl)-5-*tert*-butyl-2-hydroxybenzaldehyde, EtOH, stirred at RT for 12 h. R = *tert*-butyl. Synthesis of the precursor molecule 1c: (d)  $\text{SnCl}_4$ ,  $\text{Bu}_3\text{N}$ ,  $(\text{CH}_2\text{O})_n$ , dry toluene, reflux; (e) 35% formaldehyde, conc HCl, RT, and (f) dibenzylamine,  $\text{Et}_3\text{N}$ , THF, RT.

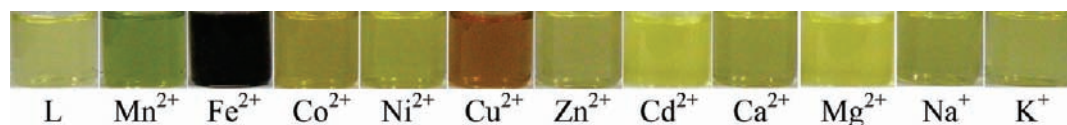


Figure 1. Visual color changes observed when  $\text{M}^{n+}$  was added to a solution of L (0.0012 M) in 1:1 ratio in methanol.

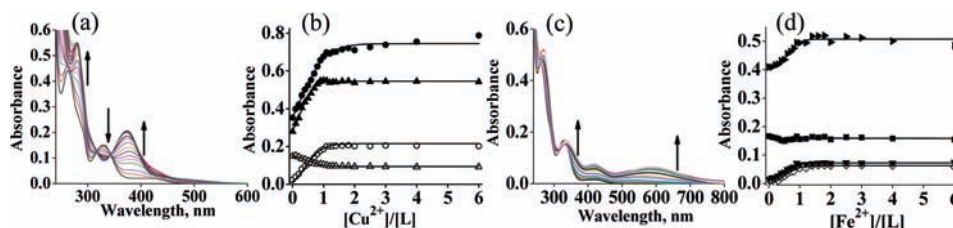


Figure 2. (a) Absorption spectral traces obtained during the titration of L (20  $\mu\text{M}$ ) in methanol with  $\text{Cu}^{2+}$  and (b) plots of absorbance versus mole ratio of  $[\text{Cu}^{2+}]/[\text{L}]$ , at 250 nm (●), 280 nm (▲), 330 nm (Δ), 375 nm (○). (c) Absorption spectral data obtained during the titration of L (20  $\mu\text{M}$ ) with  $\text{Fe}^{2+}$  and (d) plots of absorbance versus mole ratio plot of  $[\text{Fe}^{2+}]/[\text{L}]$ , at 270 nm (right-pointing triangle), 330 nm (■), 420 nm (▼), and 590 nm (◇).

by the preparation of its dinitrile and diamine derivatives. The diamine derivative, **2**, has been condensed with the aldehyde derivative,<sup>24</sup> **1c**, in methanol resulting in the formation of **L** in good yield. In turn, **1c** has been synthesized in three steps starting from *p*-*tert*-butylphenol (Scheme 1). All the precursors and the final receptor molecule, **L**, have been characterized satisfactorily by analytical and spectral methods (Experimental Section and Supporting Information). The receptor **L** exists in cone conformation which is evident from the NMR studies. The possible metal ion coordination sites present in **L** are  $\text{N}_2\text{O}_4$ ,  $\text{N}_2\text{O}_2$ ,  $\text{N}_2\text{O}_6$ , and  $\text{N}_4\text{O}_2$ , and hence **L** is a suitable receptor to explore its selectivity toward biologically prominent essential trace metal ions, such as  $\text{Fe}^{2+}$ ,  $\text{Cu}^{2+}$ , and  $\text{Zn}^{2+}$ . Indeed, these are the three elements which are present at high concentrations and are responsible for the function of more than one-half of the metalloenzymes known even in human systems.

Since **L** possesses binding cores (Scheme 1), the ion recognition properties of **L** with biologically relevant metal ions, viz.,

$\text{Mn}^{2+}$ ,  $\text{Fe}^{2+}$ ,  $\text{Co}^{2+}$ ,  $\text{Ni}^{2+}$ ,  $\text{Cu}^{2+}$ ,  $\text{Zn}^{2+}$ ,  $\text{Cd}^{2+}$ ,  $\text{Na}^+$ ,  $\text{K}^+$ ,  $\text{Ca}^{2+}$ , and  $\text{Mg}^{2+}$ , have been studied by absorption and emission techniques, besides demonstrating visually observable color changes.

**a. Visual Color and Absorption Titrations.** In order to assess whether **L** can be of any use in the recognition of metal ions by naked eye detection, **L** was titrated with various metal ions, viz.,  $\text{Mn}^{2+}$ ,  $\text{Fe}^{2+}$ ,  $\text{Co}^{2+}$ ,  $\text{Ni}^{2+}$ ,  $\text{Cu}^{2+}$ ,  $\text{Zn}^{2+}$ ,  $\text{Cd}^{2+}$ ,  $\text{Na}^+$ ,  $\text{K}^+$ ,  $\text{Ca}^{2+}$ , and  $\text{Mg}^{2+}$ , in methanol by keeping a 1:1 mole ratio and observing the corresponding color changes (Figure 1). The yellow color of **L** was almost unaltered when titrated with ions, viz.,  $\text{Mn}^{2+}$ ,  $\text{Co}^{2+}$ ,  $\text{Ni}^{2+}$ ,  $\text{Zn}^{2+}$ ,  $\text{Cd}^{2+}$ ,  $\text{Ca}^{2+}$ ,  $\text{Mg}^{2+}$ ,  $\text{Na}^+$ , and  $\text{K}^+$ ; however, it changes to pale brown in the presence of  $\text{Cu}^{2+}$  and dark blue/black in the presence of  $\text{Fe}^{2+}$ .

In order to support the visually observed color changes, absorption titrations were carried out between **L** and  $\text{Cu}^{2+}$  or  $\text{Fe}^{2+}$ . With  $\text{Cu}^{2+}$ , **L** showed four absorption peaks with their  $\lambda_{\text{max}}$  values present at 375, 330, 280, and 250 nm (Figure 2a), and the corresponding changes observed in the absorbance with respect

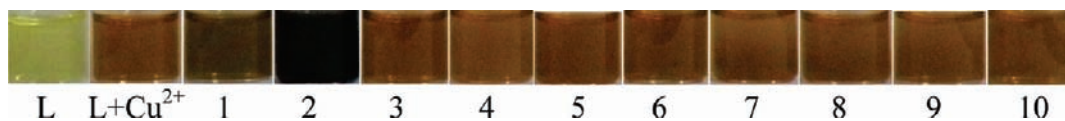


**Figure 3.** Color of the methanolic solutions of **L** (0.0012 M) obtained during the competitive ion titration of  $[L + M^{n+}]$  in a mole ratio of 1:2 with 1 equiv addition of  $Cu^{2+}$ . Here, 1 =  $Mn^{2+}$ , 2 =  $Fe^{2+}$ , 3 =  $Co^{2+}$ , 4 =  $Ni^{2+}$ , 5 =  $Zn^{2+}$ , 6 =  $Cd^{2+}$ , 7 =  $Na^+$ , 8 =  $K^+$ , 9 =  $Ca^{2+}$ , 10 =  $Mg^{2+}$ .

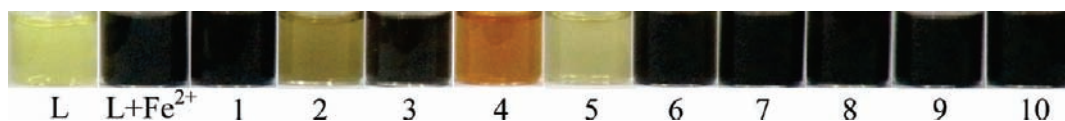


**Figure 4.** Color of the methanolic solutions of **L** (0.0012 M) obtained during the competitive ion titration of  $[L + M^{n+}]$  in a mole ratio of 1:2 with 1 equiv addition of  $Fe^{2+}$ . Here, 1 =  $Mn^{2+}$ , 2 =  $Co^{2+}$ , 3 =  $Ni^{2+}$ , 4 =  $Cu^{2+}$ , 5 =  $Zn^{2+}$ , 6 =  $Cd^{2+}$ , 7 =  $Na^+$ , 8 =  $K^+$ , 9 =  $Ca^{2+}$ , 10 =  $Mg^{2+}$ .

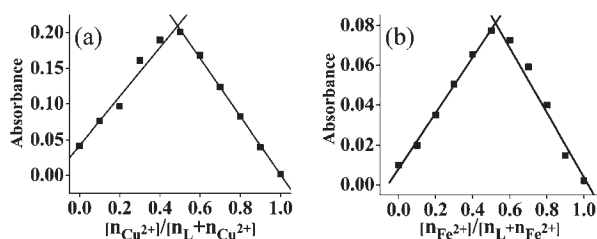


**Figure 5.** Job's plots for (a)  $Cu^{2+}$  and (b)  $Fe^{2+}$  as studied in methanol, where  $n_L$ ,  $n_{Cu^{2+}}$ , and  $n_{Fe^{2+}}$  are the mole fractions of **L**,  $Cu^{2+}$ , and  $Fe^{2+}$ , respectively.

to the mole ratio of  $[Cu^{2+}]/[L]$  can be seen from Figure 2b. The data suggests the binding of  $Cu^{2+}$ . When **L** was titrated with  $Cu^{2+}$ , the initial absorbance observed for **L** at 330 nm decreases gradually, while a new band is observed at 375 nm. Two isosbestic points were also observed at 317 and 443 nm during the titration (Figure 2a,b).

During the titration of **L** with  $Fe^{2+}$ , two new bands grew gradually as a function of increase in  $[Fe^{2+}]/[L]$  mole ratio (Figure 2c,d). While the 330 nm band showed no change in its absorbance, the 420 nm band exhibited an increase in the absorbance upon addition of  $Fe^{2+}$ . The new band observed at 590 nm corresponds to the  $d \rightarrow d$  transition. On the basis of further experiments, it has been found that **L** detects  $Cu^{2+}$  and  $Fe^{2+}$  colorimetrically by naked eye even down to a concentration of  $4.51 \pm 0.53$  and  $3.96 \pm 0.42$  ppm, respectively.

**Competitive Titration.** The recognition ability of the receptor, **L**, toward  $Fe^{2+}$  and  $Cu^{2+}$  has been studied in the presence of other competing ions. These titrations were carried out by keeping the mole ratio of **L** and  $M^{n+}$  at 1:2 followed by monitoring the color change after the addition of 1 equiv of  $Cu^{2+}$ . It has been found that **L** can detect  $Cu^{2+}$  even in the presence of other competing ions, except for  $Fe^{2+}$  (Figure 3). Similar experiments carried out in the case of  $Fe^{2+}$  indicate that **L** can detect  $Fe^{2+}$  selectively in the presence of different metal ions except for  $Co^{2+}$ ,  $Cu^{2+}$ , and  $Zn^{2+}$  (Figure 4).

The competitive ion titrations suggest the ability of **L** to detect  $Cu^{2+}$  colorimetrically even in the presence of other ions as compared to  $Fe^{2+}$ , where more than one ion interferes. Even the titration of  $\{L + Cu^{2+}\}$  with other  $M^{n+}$  resulted in no color change (Supporting Information). Similarly, the titration of  $\{L + Fe^{2+}\}$  with other  $M^{n+}$  suggests that no other metal ion would interfere with  $Fe^{2+}$  if **L** were loaded with this ion initially (Supporting Information).

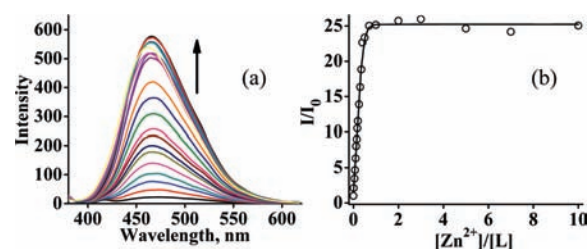


**Figure 6.** (a) Fluorescence spectral traces obtained during the titration of **L** ( $10 \mu M$ ) with  $Zn^{2+}$  in methanol and (b) plot of relative fluorescence intensity ( $I/I_0$ ) versus the mole ratio of  $[Zn^{2+}]/[L]$ , where  $I_0$  and  $I$  correspond to the fluorescence intensity of simple **L** and that observed after each addition of  $Zn^{2+}$ , respectively.

The stoichiometry of the complex of **L** with  $Cu^{2+}$  or with  $Fe^{2+}$  has been derived using continuous variation method (Job's plot). During the titration, the total concentration of **L** and  $M^{2+}$  were kept constant by varying the mole fraction of the guest,  $[M^{2+}]/[L]$ , and the plot clearly suggests the formation of a 1:1 complex (Figure 5).

Therefore, **L** provides visual color changes to detect  $Cu^{2+}$  and  $Fe^{2+}$  among the other biologically relevant ions. When any  $M^{n+}$  is added to **L** initially, the  $Cu^{2+}$  detection is challenged only by  $Fe^{2+}$ , whereas  $Fe^{2+}$  detection is being challenged by  $Co^{2+}$ ,  $Cu^{2+}$ , or  $Zn^{2+}$ . However, when  $Cu^{2+}$  or  $Fe^{2+}$  was added to **L** prior to the addition of other  $M^{n+}$ , the original color of  $\{L + Cu^{2+}\}$  or  $\{L + Fe^{2+}\}$  persists.

**b. Fluorescence Titrations.** Fluorescence titrations were carried out in methanol by exciting **L** at 370 nm and observing its emission in the region 380–620 nm. The fluorescence titration of **L** with  $Zn^{2+}$  resulted in an increase in the intensity by  $\sim 22$ – $25$ -fold (Figure 6a,b). When  $Zn^{2+}$  binds to the imine and phenolic part of **L**, the photoelectron transfer from the imine nitrogen to the salicylyl part will be blocked, and hence, a fluorescence enhancement is observed.

Among the other  $M^{n+}$  ions, only  $Fe^{2+}$ ,  $Ni^{2+}$ , and  $Cu^{2+}$  exhibited a minimal fluorescence quenching, and this was not considered as a result of low fluorescence intensity of **L**. The fluorescence intensity of **L** was unaffected by the addition of other  $M^{n+}$  ions, viz.,  $Mn^{2+}$ ,  $Co^{2+}$ ,  $Na^+$ ,  $K^+$ ,  $Ca^{2+}$ , and  $Mg^{2+}$ , while a minimal fluorescence enhancement was observed with  $Cd^{2+}$  (Figure 7). Therefore, the enhancement in the fluorescence intensity during  $Zn^{2+}$  titration was indicative of the binding of  $Zn^{2+}$  to **L**, and this switch-on behavior helps **L** to identify  $Zn^{2+}$

among the other biologically relevant  $M^{n+}$  ions studied. The association constant of L with  $Zn^{2+}$  was found to be  $49\,300 \pm 5\,200$  as determined on the basis of the Benesi–Hildebrand equation. A minimum concentration of  $\sim 45 \pm 4$  ppb ( $6.9 \times 10^{-7} \mu M$ ) of  $Zn^{2+}$  has been detected by fluorescence studies carried out by keeping L and  $Zn^{2+}$  at 1:1 and making appropriate dilutions (Supporting Information).

**Competitive Metal Ion Titration.** The practical applicability of L as a sensor for  $Zn^{2+}$  has been examined by carrying out competitive ion titrations. During the titration, L to  $M^{n+}$  has been kept constant at a 1:5 ratio in the cases of  $Mn^{2+}$ ,  $Fe^{2+}$ ,  $Co^{2+}$ ,  $Ni^{2+}$ ,  $Cu^{2+}$ ,  $Cd^{2+}$ ,  $Na^+$ ,  $K^+$ ,  $Ca^{2+}$ , and  $Mg^{2+}$ , and the resulting solutions were titrated with different mole ratios of  $Zn^{2+}$ . It has been found that  $Zn^{2+}$  replaces all the  $M^{n+}$  ions except  $Cu^{2+}$  from the binding pocket of L. Nearly a 7-fold enhancement was observed when a mixture of  $\{L + Fe^{2+}\}$  was titrated with  $Zn^{2+}$ , when compared to all other  $M^{n+}$  ions. This implies that while  $Cu^{2+}$  is highly effective in preventing the formation of the  $Zn^{2+}$  complex, the  $Fe^{2+}$  is only one-third as effective as that of  $Cu^{2+}$ . It is therefore concluded that L can be used as a sensor for  $Zn^{2+}$  even in the presence of other  $M^{n+}$  ions except for only  $Cu^{2+}$  (Figure 8).

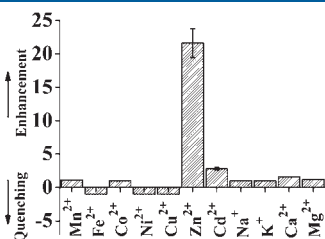


**Figure 7.** Histogram showing the number of times of enhancement or quenching of L ( $10 \mu M$ ) with  $M^{n+}$  during the fluorescence titration in methanol.

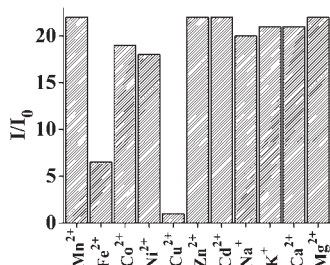


**Figure 8.** Histogram showing the changes in  $(I/I_0)$  during the addition of  $Zn^{2+}$  to a solution containing L ( $10 \mu M$ ) and  $M^{n+}$  as 1:5 ratio in the cases of  $Mn^{2+}$ ,  $Fe^{2+}$ ,  $Co^{2+}$ ,  $Ni^{2+}$ ,  $Cu^{2+}$ ,  $Cd^{2+}$ ,  $Na^+$ ,  $K^+$ ,  $Ca^{2+}$ , and  $Mg^{2+}$  in methanol.

**Absorption Titrations with  $Zn^{2+}$ .** During the titration of L with  $Zn^{2+}$ , four isosbestic points were observed at 340, 295, 270, and 255 nm suggesting its binding (Figure 9a). The absorbance of 330 nm band of L decreases with  $\lambda_{max}$  being shifted by  $\sim 30$  nm toward red upon interaction with  $Zn^{2+}$ . The bands observed at 262 and 278 nm also show concomitant changes in the absorption spectra of L in the presence of  $Zn^{2+}$  (Figure 9b). L forms a 1:1 stoichiometric complex with  $Zn^{2+}$  as evident from the Job's plot (Figure 9c). On the basis of the Benesi–Hildebrand equation, the association constants were found to be  $53\,303 \pm 3\,884$ ,  $41\,341 \pm 1\,529$ , and  $26\,844 \pm 1\,957 M^{-1}$  for  $Cu^{2+}$ ,  $Zn^{2+}$ , and  $Fe^{2+}$ , respectively. This follows the classical Irving–William order of stability, viz.,  $Fe^{2+} < Cu^{2+} > Zn^{2+}$ .

*c. Anion Binding Properties of the in Situ Generated [ZnL] Complex.* Owing to the fluorescence enhancement of L with  $Zn^{2+}$ , the in situ prepared  $Zn^{2+}$  complex of L has been subjected to study its anion binding properties in methanol. The anions tested for the studies were  $F^-$ ,  $Cl^-$ ,  $Br^-$ ,  $I^-$ ,  $ClO_4^-$ ,  $BF_4^-$ ,  $AcO^-$ ,  $SCN^-$ ,  $CO_3^{2-}$ ,  $NO_3^-$ ,  $SO_4^{2-}$ ,  $H_2PO_4^-$ ,  $HPO_4^{2-}$ , and  $P_2O_7^{4-}$ . When  $[ZnL]$  has been titrated with different anions, these anions did not exhibit any change in the fluorescence intensity of  $[ZnL]$ , while the phosphate based anions  $H_2PO_4^-$ ,  $HPO_4^{2-}$ , and  $P_2O_7^{4-}$  showed large quenching (Figure 10). During the titration, the initial fluorescence intensity of  $[ZnL]$  starts decreasing as a function of increasing concentration of phosphates and reaches a saturation point after the addition of 2 equiv. The decrease in the fluorescence intensity observed upon the addition of phosphates is attributable to the interaction of  $Zn^{2+}$  at the binding core, on the basis of fluorescence spectroscopy. The minimum concentration of  $HPO_4^{2-}$  that can be detected by  $[ZnL]$  has been found to be  $247 \pm 25$  ppb (Supporting Information).

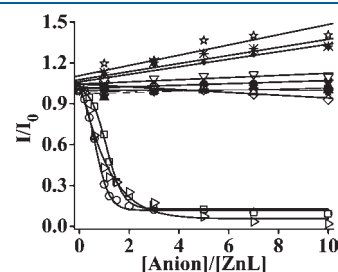


**Figure 10.** Plot of relative fluorescence intensity ( $I/I_0$ ) of  $[ZnL]$  versus the mole ratio of anions added. The symbols corresponds to  $\blacksquare = F^-$ ,  $\bullet = Cl^-$ ,  $\blacktriangle = Br^-$ ,  $\blacktriangledown = I^-$ ,  $\star = ClO_4^-$ ,  $\diamond = BF_4^-$ ,  $\blacklozenge = AcO^-$ ,  $\nabla = SCN^-$ ,  $\star = CO_3^{2-}$ ,  $\Delta = NO_3^-$ ,  $\ast = SO_4^{2-}$ ,  $\circ = H_2PO_4^-$ ,  $\square = HPO_4^{2-}$ , right-pointing triangle =  $P_2O_7^{4-}$ . The concentration of L and  $Zn^{2+}$  were kept at  $10 \mu M$  during the titration in methanol.

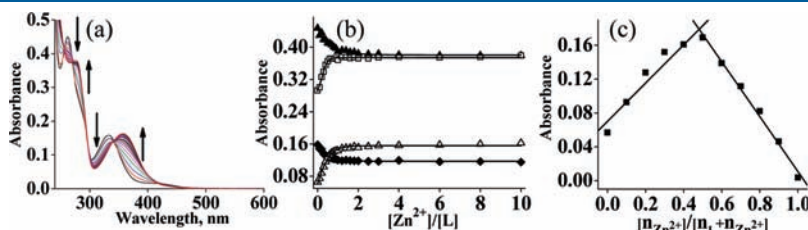


**Figure 9.** Absorption spectral data obtained during the titration of L with  $Zn^{2+}$  in methanol: (a) spectral traces of L ( $20 \mu M$ ) with  $Zn^{2+}$ , (b) plot of absorbance versus mole ratio of  $[Zn^{2+}]/[L]$  (the symbols correspond to  $\Delta = 360$  nm,  $\blacklozenge = 332$  nm,  $\square = 278$  nm,  $\blacktriangle = 262$  nm), and (c) the Job's plot for  $Zn^{2+}$ . Here,  $n_L$  and  $n_{Zn^{2+}}$  are the mole fractions of L and  $Zn^{2+}$ , respectively.

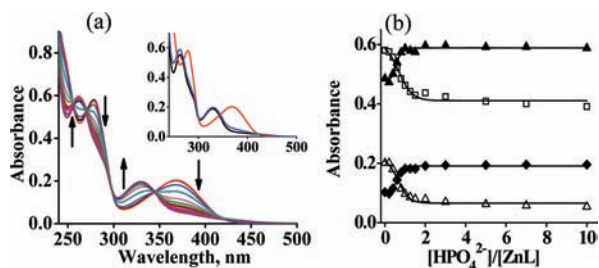


**Figure 11.** Absorption spectral data for the titration of  $[\text{ZnL}]$  with  $\text{HPO}_4^{2-}$  in methanol: (a) Spectra obtained during the titration; inset shows the absorption spectral traces corresponds to **L** (black),  $[\text{ZnL}]$  (red), and  $\{[\text{ZnL}] + \text{HPO}_4^{2-}\}$  (blue). (b) Plots of absorbance vs mole ratio of  $\text{HPO}_4^{2-}$  added. The symbols corresponds to  $\Delta = 370$  nm,  $\blacklozenge = 328$  nm,  $\square = 278$  nm,  $\blacktriangle = 262$  nm. The concentration of **L** and  $\text{Zn}^{2+}$  were  $20 \mu\text{M}$  during the titration.

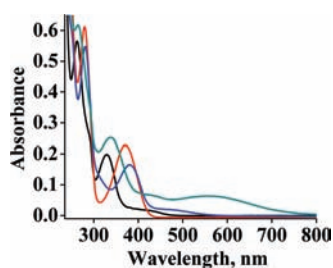


**Figure 12.** Absorption spectral traces of **L** and its isolated complexes of zinc, copper, and iron. The peaks correspond to **L** = black, **3** = red, **4** = blue, and **5** = green. The concentrations of **L** and all the other complexes were kept as  $1.67 \times 10^{-5}$  M in  $\text{CH}_3\text{OH}/\text{CHCl}_3$  (12:1 v/v).

To get more insights into the phosphate binding, absorption spectral titrations were carried out between  $[\text{ZnL}]$  and different phosphates. It has been found that the initial absorbance band of  $[\text{ZnL}]$  has been shifted from 370 and 278 nm to 330 and 262 nm, respectively, upon the addition of  $\text{HPO}_4^{2-}$ , and finally the absorption spectrum shows characteristics similar to that of the simple **L** (Figure 11). Similar results have been observed for both  $\text{H}_2\text{PO}_4^-$  and  $\text{P}_2\text{O}_7^{4-}$  (Supporting Information). These results indicate that the titration of  $[\text{ZnL}]$  with phosphate is exactly the reverse of the titration of **L** with  $\text{Zn}^{2+}$ .

*d. Isolation and Characterization of the Complexes.* Reaction of **L** with the salts of  $\text{Zn}^{2+}$ ,  $\text{Cu}^{2+}$ , and  $\text{Fe}^{2+}$  resulted in the corresponding complexes **3**, **4**, and **5**, respectively (Supporting Information). These were characterized by elemental analysis, absorption, IR, and mass spectrometry. In the IR spectrum, the peaks corresponding to  $\nu_{\text{C}=\text{N}}$  and  $\nu_{\text{OH}}$  exhibited significant changes upon complexation. The peak corresponding to  $\nu_{\text{C}=\text{N}}$  of the free **L** has been shifted from 1633 to 1616, 1620, and 1617  $\text{cm}^{-1}$ , respectively, in the cases of **3**, **4**, and **5**. Similarly,  $\nu_{\text{OH}}$  has been shifted to the 3388 and 3438  $\text{cm}^{-1}$  from the simple **L** (3397  $\text{cm}^{-1}$ ) for **3** and **4**, respectively. This suggests the involvement of both imine and phenolic  $-\text{OH}$  groups in the metal ion coordination. The absorption spectra of simple **L** and its complexes **3**, **4**, and **5** have been recorded (Figure 12). The absorption band of **L** (262, 330 nm) has been shifted when it formed complexes with zinc (280, 372 nm), copper (281, 382 nm), and iron (265, 338 nm) in addition to the formation of a new band in the case of the iron complex at 560 nm. The elemental analysis fits well with a 1:1 complex in all the three

**Table 1.** Crystallographic Parameters for the Structure Determination and Refinement

	3	4
empirical formula	$\text{C}_{102}\text{H}_{118}\text{N}_4\text{O}_{12}\text{Zn}$	$\text{C}_{108}\text{H}_{130}\text{N}_8\text{O}_9\text{Cu}$
MW	1657.37	1747.74
<i>T</i> (K)	120(2)	150(2)
cryst syst	monoclinic	triclinic
space group	$P2_1/n$	$P\bar{1}$
<i>a</i> /Å	13.3294(16)	13.9951(4)
<i>b</i> /Å	21.9714(18)	19.5154(10)
<i>c</i> /Å	32.721(2)	22.0745(8)
$\alpha$ /deg	90.000	112.528(4)
$\beta$ /deg	91.074(8)	93.922(2)
$\gamma$ /deg	90.000	109.911(3)
<i>V</i> /Å <sup>3</sup>	9581.2(15)	5096.9(4)
<i>Z</i>	4	2
abs coeff ( $\text{mm}^{-1}$ )	0.316	0.273
<i>D<sub>c</sub></i> /g $\text{cm}^{-3}$	1.149	1.139
reflns collected	79 174	38 365
unique reflns	16 839	17 899
<i>R<sub>int</sub></i>	0.226	0.039
params	1098	1165
final <i>R</i> [ <i>I</i> > 2σ( <i>I</i> )]	0.0832	0.0625
w <i>R</i> 2	0.2393	0.2131

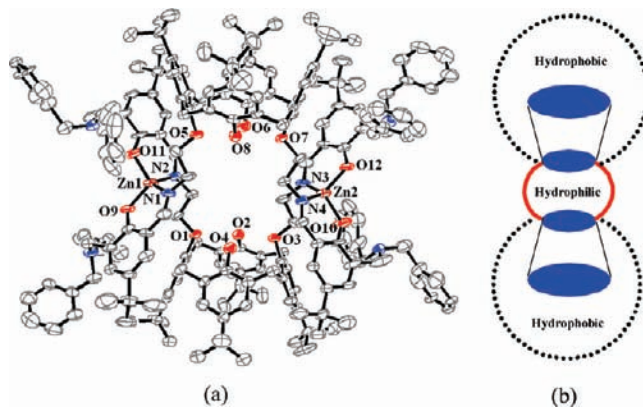


**Figure 13.** (a) X-ray diffracted crystal structure of the zinc complex of **L**, **3**, and (b) pictorial representation of the hydrophobic and hydrophilic part present in **3** by monitoring the adjacent molecules.

cases and was further supported by ESI MS or MALDI-TOF wherein the presence of the metal ion could be identified on the basis of an isotope peak pattern in the cases of **3**, **4**, and **5**. The molecular ion peak (*m/z*) observed for **3** at 3074.85 corresponds to a 2:2 complex between **L** and zinc, while that observed in the cases of **4** and **5** at 1535.68 and 1527.73, respectively, indicates the formation of a 1:1 complex. Since we could not isolate the single crystals of the iron complex, powder XRD spectra of **L** as well as of the isolated complexes were measured, and the crystallinities were compared (Supporting Information).

The zinc complex, **3**, crystallizes from a mixture of chloroform and methanol to give single crystals of diffraction quality. The details of the data collection and the structure refinement are given in Table 1.

Table 2. Important Bond Distances and Dihedral Angles of 3 and 4

3	angle (deg)/distance (Å)	4	angles (deg)/distance (Å)
N2–Zn1–O11/Zn1–N1	94.591(23)/1.963(5)	N1–Cu–N2/Cu–O1	166.97 (12)/1.90 (3)
N2–Zn1–N1/Zn1–N2	110.547(22)/1.980(5)	N1–Cu–O2/Cu–O2	90.13 (12)/1.90 (2)
N2–Zn1–O9/Zn1–O9	125.527(19)/1.907(4)	N1–Cu–O1/Cu–N1	91.66 (12)/1.98 (3)
O9–Zn1–N1/Zn1–O11	96.492(22)/1.898(5)	O1–Cu–O2/Cu–N2	157.58 (13)/1.98 (33)
O9–Zn1–O11	106.981(22)	O1–Cu–N2	90.61 (12)
N1–Zn1–O11	125.533(23)	N2–Cu–O2	92.66 (12)

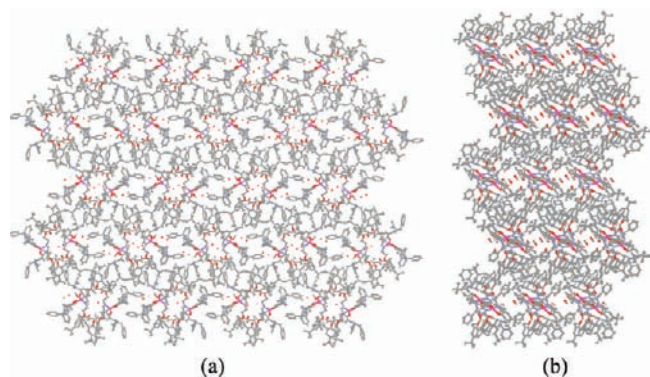


Figure 14. Lattice structure of Zn<sup>2+</sup> complex (a) viewed along *a*-axis (b) viewed along *b*-axis.

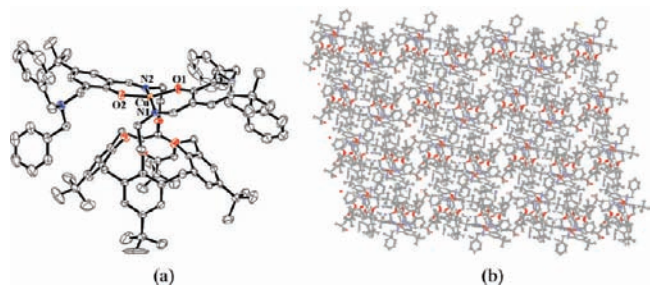


Figure 15. (a) ORTEP diagram of crystal structure of the Cu<sup>2+</sup> complex of L, 4 at 50% ellipsoid probability and (b) lattice structure of Cu<sup>2+</sup> complex viewed along *b*-axis.

The structure of 3 (Figure 13a) is a covalent 2:2 dimer, viz., [ZnL]<sub>2</sub>, possessing a center of symmetry. The calix[4]arene portion exhibits a cone conformation in its crystal structure, that is stabilized by two strong intramolecular hydrogen bonds of the type O–H<sub>phe</sub>···O<sub>et</sub> at the lower rim. The dimer was formed by joining two [ZnL] entities in a head-to-head fashion. Each Zn<sup>2+</sup> center exhibits a distorted tetrahedral geometry with N<sub>2</sub>O<sub>2</sub> binding core where the arm of each calixarene extends NO bidentate chelate from its imino-phenolic center. The two Zn<sup>2+</sup> centers are farther apart by 0.94 nm. The metric data for the coordination sphere are given in Table 2 (Supporting Information). The dimeric Zn<sup>2+</sup> complex exhibits an open intracomplex cavity that is reasonably spherical in nature at the junction of the two lower rims and possesses hydrophilic interior lining and thus results in a nanocavity of the dimensions 0.85 × 0.75 nm<sup>2</sup> (third dimension being open). The complex is mostly surrounded by hydrophobic fencing as can be seen from the cartoon picture shown in Figure 13b.

In the lattice of 3, the dinuclear zinc complex units are stacked one over the other to form columns resulting in the formation intercolumnar cavity besides the cavity found within the complex (Figure 14). While the intracomplex cavity is filled with the solvent molecules, the intercolumnar cavities possess both the solvent as well as aromatic moieties protruding from the calixarene arms. Thus, the lattice of 3 exhibits layers of hydrophobic (~1.2 nm) and hydrophilic (~0.85 nm) ones.

The copper complex of L resulted in single crystals of diffraction quality by slow evaporation of the acetonitrile solution. The crystals were found to be triclinic-centrosymmetric and possess three acetonitrile and three water molecules per L in the lattice. The details of the data collection and the structure refinement are given in Table 1 (Supporting Information). Similar to 3, calix[4]arene exists in cone conformation even after the complexation by the involvement of intramolecular hydrogen bonds formed between the free phenolic –OH's and the substituted arms. The Cu<sup>2+</sup> has distorted square planar geometry with N<sub>2</sub>O<sub>2</sub> core where each arm acts as a NO chelate center using imino-phenol moiety and thus exists as monomer unlike the case of the zinc complex (Figure. 15). The metric data for the coordination sphere has been given in Table 2. The close vicinity of the Cu<sup>2+</sup> coordination sphere exhibits bowl shape structure at the lower rim with hemispherical opening for external agents to enter from the top of the lower rim. In the lattice, the complex molecules form columnar structure by stacking one over the other. In the neighbor column, the complexes were arranged exactly in an opposite direction. The solvent molecules fill the intercolumnar spaces besides the presence of acetonitrile in the arene cavity of each of the calixarene unit.

## CONCLUSIONS AND CORRELATIONS

The conjugate of calix[4]arene, L, visually detects Cu<sup>2+</sup> and Fe<sup>2+</sup> among all the other ions studied. It senses Cu<sup>2+</sup> even in the presence of other ions but in the absence of Fe<sup>2+</sup>, while the detection of Fe<sup>2+</sup> decreases in the presence of Co<sup>2+</sup>, Cu<sup>2+</sup>, and Zn<sup>2+</sup>, which suggests high selectivity of L toward Cu<sup>2+</sup> as compared to Fe<sup>2+</sup>. L detects Cu<sup>2+</sup> and Fe<sup>2+</sup> visually even down to a concentration of 4.51 ± 0.53 and 3.96 ± 0.42 ppm, respectively. Absorption titrations have been carried out to support the Cu<sup>2+</sup> and Fe<sup>2+</sup> binding. From all the fluorescence studies discussed in this paper, it can be concluded that the conjugate of calix[4]arene possessing salicylimine and dibenzyl amine moieties together acts as sensor for Zn<sup>2+</sup> by fluorescence enhancement with a minimum detection limit of 45 ± 4 ppb. Therefore, L acts as a fluorescence switch-on sensor toward Zn<sup>2+</sup>. The ability of L to detect Zn<sup>2+</sup> even in the presence of other biologically relevant M<sup>n+</sup> species has been checked by carrying out competitive titrations. The absorption spectra were characteristic of the formation of the complex between Zn<sup>2+</sup> and L.

The 1:1 stoichiometry of the complex formed between the L and  $Zn^{2+}$ ,  $Cu^{2+}$ , or  $Fe^{2+}$  has been demonstrated by Job's plot. However, when this complex was crystallized with  $Zn^{2+}$ , it exhibits a dimer, viz.,  $[ZnL]_2$ , and the corresponding 2:2 complex of zinc has been further characterized by MALDI-TOF and elemental analysis. The in situ prepared  $[ZnL]$  detects phosphates with a detection limit of  $247 \pm 25$  ppb. To our knowledge, L is the first receptor to be effective toward three essential transition ions of biology, viz.,  $Fe^{2+}$ ,  $Cu^{2+}$ , and  $Zn^{2+}$  using two different techniques.

The structure of  $[ZnL]_2$  complex has been established by single crystal XRD, and two of the  $Zn^{2+}$  ions bring both the calix[4]arene derivatives together to form a nanocore with polar interior. The copper complex of L was found to be 1:1, and this has been well characterized by mass spectrometry and elemental analysis. Also, the structure has been established by single crystal X-ray diffraction. The powder XRD of the iron complex of L indicates the noncrystallinity of the complex similar to that observed even with simple L. The powder XRD data of L and its complexes shows the crystalline nature of 3 and 4 and the noncrystalline nature of L and 5.

## ■ ASSOCIATED CONTENT

**S** Supporting Information. Synthesis and characterization of precursor molecules, spectral data of L,  $^1H$  NMR spectra of 3, competitive color change experiments, minimum detection limit, spectral and XRD data of complexes, absorption spectral titration of  $[ZnL]$  with phosphates, and powder XRD studies. This material is available free of charge via the Internet at <http://pubs.acs.org>.

## ■ AUTHOR INFORMATION

### Corresponding Author

\*E-mail: [cprao@iitb.ac.in](mailto:cprao@iitb.ac.in). Phone: 91 22 2576 7162. Fax: 91 22 2572 3480.

## ■ ACKNOWLEDGMENT

C.P.R. acknowledges the financial support by DST, CSIR, and BRNS-DAE. R.J. thanks UGC, and J.P.C. thanks CSIR, for the research fellowships.

## ■ REFERENCES

- (1) Jiang, P.; Guo, Z. *Coord. Chem. Rev.* **2004**, *248*, 205.
- (2) Coleman, J. E. *Curr. Opin. Chem. Biol.* **1998**, *2*, 222.
- (3) (a) Jedrzejak, M. J.; Setlow, P. *Chem. Rev.* **2001**, *101*, 607. (b) Weston, J. *Chem. Rev.* **2005**, *105*, 2151.
- (4) MacDonald, R. S. *J. Nutr.* **2000**, *130*, 1500S.
- (5) (a) Bott, A. W. *Cur. Sep.* **1999**, *18*, 47. (b) Hudson, J. M.; Heffron, K.; Kotlyar, V.; Sher, Y.; Maklashina, E.; Cecchini, G.; Armstrong, F. A. *J. Am. Chem. Soc.* **2005**, *127*, 6977.
- (6) (a) Hartzell, C.; Hansen, R.; Beinert, H. *Proc. Natl. Acad. Sci. U.S.A.* **1973**, *70*, 2477. (b) Aisen, P.; Enns, C.; Wessling-Resnick, M. *Int. J. Biochem. Cell Biol.* **2001**, *33*, 940.
- (7) Fredericksen, C. J.; Koh, J. Y.; Bush, A. I. *Nat. Rev. Neurosci.* **2005**, *6*, 449.
- (8) Weiss, J. H.; Sensi, S. L.; Koh, J. Y. *Trends. Pharmacol. Sci.* **2000**, *21*, 395.
- (9) (a) Merian, E. *Metals and Their Compounds in the Environment*; VCH: Weinheim, 1991; p 893. (b) Zietz, B. P.; Dieter, H. H.; Lakomek,

M.; Schneider, H.; Kessler-Gaedtke, B.; Dunkelberg, H. *Sci. Total Environ.* **2003**, *302*, 127.

(10) Gupta, A.; Crumbliss, A. L. *J. Lab. Clin. Med.* **2000**, 371.

(11) (a) Gao, X.; Campian, J. L.; Qian, M.; Sun, X.-F.; Eaton, J. W. *J. Biol. Chem.* **2009**, *284*, 4767. (b) Siah, C. W.; Trinder, D.; Olynyk, J. K. *Clin. Chim. Acta* **2005**, *358*, 24. (c) Conrad, M. E.; Umbreit, J. N.; Moore, E. G. *Adv. Exp. Med. Biol.* **1994**, *356*, 69.

(12) (a) Dietrich, B. *Pure Appl. Chem.* **1993**, *65*, 1457. (b) Sessler, J. L.; Gale, P. A.; Cho, W.-S. *Anion Receptor Chemistry*; Royal Society of Chemistry: Cambridge, U.K., 2006.

(13) (a) *The Biochemistry of Nucleic Acids*, 10th ed.; Adams, R. L. P., Kowner, J. T., Leader, D. P., Eds.; Chapman and Hall: New York, 1986. (b) Saenger, W. *Principles of Nucleic Acid Structure*; Springer: New York, 1998.

(14) (a) Creaven, B. S.; Donlon, D. F.; McGinley, J. *Coord. Chem. Rev.* **2009**, *253*, 893. (b) Kim, J. S.; Quang, D. T. *Chem. Rev.* **2007**, *107*, 3780.

(15) (a) Lankshear, M. D.; Dudley, I. M.; Chan, K.-M.; Cowley, A. R.; Santos, S. M.; Felix, V.; Beer, P. D. *Chem.—Eur. J.* **2008**, *14*, 2248. (b) Valeur, B.; Leray, I. *Coord. Chem. Rev.* **2000**, *205*, 3. (c) Leray, I.; Valeur, B. *Eur. J. Inorg. Chem.* **2009**, 3525. (d) Kim, J. S.; Lee, S. Y.; Yoon, J.; Vicens, J. *Chem. Commun.* **2009**, 4791. (e) de Silva, A. P.; Gunaratne, H. Q. N.; Gunnlaugsson, T.; Huxley, A. J. M.; McCoy, C. P.; Rademacher, J. T.; Rice, T. E. *Chem. Rev.* **1997**, *97*, 1515. (f) Lankshear, M. D.; Cowley, A. R.; Beer, P. D. *Chem. Commun.* **2006**, 612. (g) Gale, P. A.; Quesada, R. *Coord. Chem. Rev.* **2006**, *250*, 3219. (h) Caltagirone, C.; Gale, P. A. *Chem. Soc. Rev.* **2009**, *38*, 520. (i) Quinlan, E.; Matthews, S. E.; Gunnlaugsson, T. *J. Org. Chem.* **2007**, *72*, 7497. (j) McConnell, A. J.; Serpell, C. J.; Thompson, A. L.; Allan, D. R.; Beer, P. D. *Chem.—Eur. J.* **2010**, *16*, 1256. (k) Quinlan, E.; Matthews, S. E.; Gunnlaugsson, T. *Tetrahedron Lett.* **2006**, *47*, 9333. (l) Lee, J. Y.; Kim, S. K.; Jung, J. H.; Kim, J. S. *J. Org. Chem.* **2005**, *70*, 1463. (m) Lee, S. H.; Kim, H. J.; Lee, Y. O.; Vicens, J.; Kim, J. S. *Tetrahedron Lett.* **2006**, *47*, 4373.

(16) (a) Liu, S.-Y.; He, Y.-B.; Wu, J.-L.; Wei, L.-H.; Qin, H.-J.; Meng, L.-Z.; Hu, L. *Org. Biomol. Chem.* **2004**, *2*, 1582. (b) Koner, A. L.; Schatz, J.; Nau, W. M.; Pischel, U. *J. Org. Chem.* **2007**, *72*, 3889. (c) Perret, F.; Lazar, A. N.; Coleman, A. W. *Chem. Commun.* **2006**, 2425. (d) Arena, G.; Casnati, A.; Contino, A.; Magri, A.; Sansone, F.; Sciotto, D.; Ungaro, R. *Org. Biomol. Chem.* **2006**, *4*, 243. (e) Da Silva, E.; Coleman, A. W. *Tetrahedron* **2003**, *59*, 7357. (f) Perret, F.; Morel-Desrosiers, N.; Coleman, A. W. *J. Supramol. Chem.* **2002**, *2*, 533. (g) Lazar, A. N.; Navaza, A.; Coleman, A. W. *Chem. Commun.* **2004**, 1052. (h) Lazar, A. N.; Danylyuk, O.; Suwinska, K.; Coleman, A. W. *New J. Chem.* **2006**, *30*, 59. (i) Coleman, A. W.; Silva, E. D.; Nouar, F.; Nierlich, M.; Navaza, A. *Chem. Commun.* **2003**, 826. (j) Acharya, A.; Ramanujam, B.; Chinta, J. P.; Rao, C. P. *J. Org. Chem.* **2011**, *76*, 127. (k) Bandela, A.; Chinta, J. P.; Hinge, V. K.; Dikundwar, A. G.; Guru Row, T. N.; Rao, C. P. *J. Org. Chem.* **2011**, *76*, 1742.

(17) (a) Cacciapaglia, R.; Casnati, A.; Mandolini, L.; Reinhoudt, D. N.; Salvio, R.; Sartori, A.; Ungaro, R. *J. Org. Chem.* **2005**, *70*, 624. (b) Cacciapaglia, R.; Casnati, A.; Mandolini, L.; Reinhoudt, D. N.; Salvio, R.; Sartori, A.; Ungaro, R. *J. Am. Chem. Soc.* **2006**, *128*, 12322. (c) Cacciapaglia, R.; Casnati, A.; Mandolini, L.; Reinhoudt, D. N.; Salvio, R.; Sartori, A.; Ungaro, R. *J. Org. Chem.* **2005**, *70*, 5398. (d) Bakirci, H.; Koner, A. L.; Dickman, M. H.; Kortz, U.; Nau, W. M. *Angew. Chem., Int. Ed.* **2006**, *45*, 7400. (e) Ozturk, G.; Akkaya, E. U. *Org. Lett.* **2004**, *6*, 241.

(18) (a) Bagatin, I. A.; de Souza, E. S.; Ito, A. S.; Toma, H. E. *Inorg. Chem. Commun.* **2003**, *6*, 288. (b) Unob, F.; Asfari, Z.; Vicens, J. *Tetrahedron Lett.* **1998**, *39*, 2951. (c) Cao, Y.-D.; Zheng, Q.-Y.; Chen, C.-F.; Huang, Z.-T. *Tetrahedron Lett.* **2003**, *44*, 4751. (d) Dessingou, J.; Joseph, R.; Rao, C. P. *Tetrahedron Lett.* **2005**, *46*, 7967. (e) Joseph, R.; Ramanujam, B.; Pal, H.; Rao, C. P. *Tetrahedron Lett.* **2008**, *49*, 6257. (f) Pathak, R. K.; Ibrahim, S. M.; Rao, C. P. *Tetrahedron Lett.* **2009**, *50*, 2730. (g) Park, S. Y.; Yoon, J. H.; Hong, C. S.; Souane, R.; Kim, J. S.; Matthews, S. E.; Vicens, J. *J. Org. Chem.* **2008**, *73*, 8212. (h) Pathak, R. K.; Dikundwar, A. G.; Row, T. N. G.; Rao, C. P. *Chem. Commun.* **2010**, 4345. (i) Joseph, R.; Chinta, J. P.; Rao, C. P. *J. Org. Chem.* **2010**, *75*, 3387. (j) Li, G.-Ke.; Xu, Z.-X.; Chen, C.-F.; Huang, Z.-T. *Chem.*



- Commun.* **2008**, 1774. (k) Bodenant, B.; Weil, T.; Businelli-Pourcel, M.; Fages, F.; Barbe, B.; Pianet, I.; Laguerr, M. *J. Org. Chem.* **1999**, *64*, 7034. (l) Liu, J.-M.; Zheng, Q.-Y.; Yang, J.-L.; Chen, C.-F.; Huang, Z.-T. *Tetrahedron Lett.* **2002**, *43*, 9209. (m) Cao, Y.-D.; Zheng, Q.-Y.; Chen, C.-F.; Huang, Z.-T. *Tetrahedron Lett.* **2003**, *44*, 4751. (n) Chang, K.-C.; Luo, L.-Y.; Diau, E. W.-G.; Chung, W.-S. *Tetrahedron Lett.* **2008**, *49*, 5013. (o) Quang, D. T.; Jung, H. S.; Yoon, J. H.; Lee, S. Y.; Kim, J. S. *Bull. Korean Chem. Soc.* **2007**, *28*, 682. (p) Liang, Z.; Liu, Z.; Jiang, L.; Gao, Y. *Tetrahedron Lett.* **2007**, *48*, 1629. (q) Xu, Z.; Kim, S.; Kim, H. N.; Han, S. J.; Lee, C.; Kim, J. S.; Qian, X.; Yoon, J. *Tetrahedron Lett.* **2007**, *48*, 9151. (r) Kumar, R.; Bhalla, V.; Kumar, M. *Tetrahedron* **2008**, *64*, 8095. (s) Bhalla, V.; Kumar, R.; Kumar, M.; Dhir, A. *Tetrahedron* **2007**, *63*, 11153. (t) Joseph, R.; Ramanujam, B.; Acharya, A.; Rao, C. P. *Tetrahedron Lett.* **2009**, *50*, 2735.
- (19) Zhang, J. F.; Bhuniya, S.; Lee, Y. H.; Bae, C.; Lee, J. H.; Kim, J. S. *Tetrahedron Lett.* **2010**, *51*, 3719.
- (20) (a) Senthilvelan, A.; Ho, I.-T.; Chang, K.-C.; Lee, G.-H.; Liu, Y.-H.; Chung, W.-S. *Chem.—Eur. J.* **2009**, *15*, 6152. (b) Beer, P. D.; Timoshenko, V.; Maestri, M.; Passaniti, P.; Balzani, V. *Chem. Commun.* **1999**, 1755.
- (21) (a) Watchait, S.; Kaowiew, A.; Suksai, C.; Tuntulani, T.; Ngeontae, W.; Pakawatchai, C. *Tetrahedron Lett.* **2010**, *51*, 3398. (b) Beer, P. D.; Cadman, J. *Coord. Chem. Rev.* **2000**, *205*, 131.
- (22) (a) Joseph, R.; Ramanujam, B.; Acharya, A.; Khutia, A.; Rao, C. P. *J. Org. Chem.* **2008**, *73*, 5745. (b) Joseph, R.; Ramanujam, B.; Acharya, A.; Rao, C. P. *J. Org. Chem.* **2009**, *74*, 8181.
- (23) (a) Collins, E. M.; McKervey, M. A.; Madigan, E.; Moran, M. B.; Owens, M.; Ferguson, G.; Harris, S. J. *J. Chem. Soc., Perkin Trans. 1* **1991**, 3137. (b) Joseph, R.; Gupta, A.; Rao, C. P. *Indian J. Chem., Sect A: Inorg., Bio-inorg., Phys., Theor. Anal. Chem.* **2007**, *46A*, 1095. (c) Zhang, W.-C.; Huang, Z.-T. *Synthesis* **1997**, 1073.
- (24) (a) Shao, N.; Zhang, Y.; Cheung, S.; Yang, R.; Chan, W.; Mo, T.; Li, K.; Liu, F. *Anal. Chem.* **2005**, *77*, 7294. (b) Wang, Q.; Wilson, C.; Blake, A. J.; Collinson, S. R.; Tasker, P. A.; Schroder, M. *Tetrahedron Lett.* **2006**, *47*, 8983. (c) Lambert, E.; Chabut, B.; Chardon-Noblat, S.; Deronzier, A.; Chottard, G.; Bousseksou, A.; Tuchagues, J.-P.; Laugier, J.; Bardet, M.; Latour, J.-M. *J. Am. Chem. Soc.* **1997**, *119*, 9424.